COASTAL ZONE MONITORING BY CHRIS/PROBA: FROM CAL/VAL ACTIVITIES TO BIOGEOPHYSICAL PARAMETERS ASSESSMENT

A. Barducci, D. Guzzi, P. Marcoionni, I. Pippi
CNR – IFAC, Via Madonna del Piano 10, 50019 Sesto Fiorentino, Italy
(i.pippi, d.guzzi)@ifac.cnr.it, a.barducci@aliceposta.it, p.marcoionni@iccolor.it

KEY WORDS: CHRIS/PROBA, Remote sensing, Coastal zone monitoring, Calibration, Validation

ABSTRACT:

CHRIS hyperspectral sensor has been operating since 2003 on board of the PROBA-1 satellite. Many areas around the world have been imaged by this sensor, among them San Rossore Natural Park (Italy) in the framework of the Cat.1 LBR ESA-EOPI Project ID.2832. The west end of the Park, characterised by pine-forest, is limited by the Tyrrhenian sea, while in the southern part is present a wet area.
Data accumulated over seven years of overpasses allowed us to perform a multi-temporal analysis of the coastal area as well as to assess physical and biogeochemical parameters from the retrieved reflectance maps.
Cloud free images acquired by the CHRIS sensor have been processed, obtaining L1B (at-sensor radiance images) and L2 (spectral reflectance maps) data. For this purpose the received "response corrected" data sets have been firstly processed to remove the residual stripe noise affecting CHRIS data. An atmospheric correction procedure, based on MODTRAN5 radiative transfer code, has been applied to retrieve spectral reflectance maps. The satellite ability to point the observed area at five different viewing angles has allowed the investigation of bidirectional reflectance properties of natural bodies that are responsible for most of the observed texture.
In this paper we summarized our activity on CHRIS-PROBA data processing and their use for environmental investigations in order to better understand the complexity of the San Rossore ecosystem, which is representative of many Mediterranean costal zones. Particular attention was paid to accurately validate the data acquired, using the facilities available at San Rossore test site.

1. INTRODUCTION

Data collected by aerospace hyperspectral imagers can be used to improve the classification of coastal areas and assess their spatial and temporal change. To this purpose, the sensor response has to be accurately compensated by means of calibration procedures, and physical modelling of the retrieved data should be developed as to infer accurate theoretical interpretations (Ramsey, 1992).
Tuscany coastal wetlands are often considered valuable ecosystems but they are menaced by anthropogenic activities (Azzari 1999). In response to this threat, an established trend for the re-naturalization of ecosystems has brought to the re-formation of small extension wetlands, the Regional park of Migliarino, San Rossore, Massaciuccoli being an important example of this politics. The park is located on the seaside, near Pisa (Italy), and is mainly covered by pine-forest. Its southern part is the wetland area of Lame di Fuori, a system of ponds and dunes affected by the sediment deposition occurring at the river estuary.
Due to accumulation of remotely sensed and in-situ collected data, and considering the circumstance that the Park incorporates several kinds of targets and land-covers, many areas are being utilised as test-site in various remote sensing campaigns.
Since 2002 more than 35 image sets have been acquired over the San Rossore forestry test site. Among them, half are cloud-free image sets and have been completely processed (destriping, and

atmospheric correction). The provided CHRIS data sets are still affected by various inaccuracies, mainly due to the sensor calibration. To mitigate this problem the received data have to be pre-processed.
In this paper CHRIS datasets collected over the San Rossore Park has been re-examined, in order to assess the sensor performance, and investigate the Park status. In Sect. 2 our destriping algorithm is outlined and the processed CHRIS images are analysed. Sect. 3 describes the procedure adopted for carrying out the atmospheric corrections of CHRIS images, while the estimation of biogeophysical parameters characteristics of the San Rossore Park is discussed in Sect 4. Finally, Sect. 5 draws some conclusions and discuss future work.

2. DATA PRE-PROCESSING

2.1 Coherent Noise removal

The quality of the images acquired by spaceborne sensors is often affected by noise patterns and other disturbances that requires careful calibration of the instrument response. Non-periodic disturbances characterized by a high degree of spatial and spectral coherence like “stripe noise” often affect the images gathered by imaging spectrometers, and complex measurements are necessary for restoring the data. Even the CHRIS Response Corrected Image (RCI) data, provided to the scientific users along these years, are partially affected by this kind of coherent noise (striping).
An algorithm (Barducci, 2008) was specifically developed to remove coherent noise from remotely sensed images without involving flat-field calibration measurements. The algorithm utilises a subset *p* of the image Hough transformed, chosen according to the spatial structure of the considered noise pattern. For imaging spectrometers this subset is defined by all the integrals computed over image columns that produce an image profile corresponding to the average image horizontal line.
Let *g* be the raw, or radiometrically calibrated, image gathered by an imaging spectrometer device, in which x,y denote the co-ordinates of a generic pixel, and □ indicates the wavelength (of the considered spectral band). The profile *p* is defined by:

$$p(x,\lambda) = \int g(x,y,\lambda)dy \tag{1}$$

The profile *p*, which is the average image row at wavelength □, obviously holds much information concerning the spatial structure of the disturbance pattern and, as a consequence of averaging, it is scarcely influenced by random noise and target texture. We suppose that, while striping contributions rapidly change with the position x, those originated by the target texture slowly vary with x. In a different wording, we can introduce a cut-off spatial frequency f_c that roughly splits contributions due to the scene texture from those originated by striping. This means that for spatial frequency f greater than f_c the power spectrum is mainly originated from the noise pattern. As long as this supposition holds true, the noise pattern can be retrieved simply applying a high-pass filter to the profile *p* in Eq. 1. The physical likelihood of this assumption may be visually inferred from the characteristics of the raw images gathered by the sensor, and shown in Fig. 1a.
In order to extract the high frequency components of the profile *p* we have designed a two-stage filtering procedure, which has some valuable properties (Barducci, 2008). Initially, a low-pass is applied to the profile p, whose output *s* ideally contains contributions from the scene texture alone. Then the *p*-to-s ratio is assumed to be the best estimate of the noise pattern *c*, which is used to compute the corrected image *i* according to the following formulas:

$$c(x,\lambda) = \frac{s(x,\lambda\}}{p(x,\lambda)} \tag{2}$$

$$i(x, y, \lambda) = \frac{g(x, y, \lambda)}{c(x, \lambda)}$$

It should be noted that the value of the newly defined profile c oscillates around the value 1. This property gives the corrected image i two important characteristics: first, i has on average the same intensity distribution as the original data g, and images i and g have the same pixel spectra in any homogeneous scene regions. Therefore, the entire correcting procedure is suitable for processing radiometric calibrated data without affecting their physical units of measure.

(a) *(b)*

Fig. 1. CHRIS acquisition over San Rossore on August 9, 2005 (MZA = -6^o, FZA = 0^o): (a) equalized image from the provided RCI data, (b) equalized image after removing the coherent noise.

A result of the coherent-noise removal procedure is shown in Fig.1b. The algorithm's ability to preserve the averaged image brightness has been verified with accuracy to within +/- 1% of accuracy.

2.2 SNR estimation

Differently from coherent disturbances, random noise is due to a fully stochastic process. In digital images this kind of noise appears as a salt-pepper pattern, which affects the scene quality, and can't be removed without spatial resolution losses. The knowledge of random noise amplitude is important to estimate the corresponding Signal-to-Noise Ratio (SNR), to assess sensor and data quality, and to perform specific image processing algorithm (e.g. the Maximum Noise Fraction (MNF) or the Noise Adjusted Principal Components (NAPC)).
To this aim an estimation method (bit-plane method) has been developed with the essential property to be almost insensitive to scene's texture (Barducci, 2005). The algorithm is based on the assumption that noise statistics is spatially stationary and not auto-correlated. The central idea of our algorithm is to extract from every image the corresponding bit-plane sequence starting from the most significant bit (MSB) down to the less significant one (LSB), and to establish if the bit-plane obeys a random distribution. To this aim the difference $\Delta_i(x, y, k)$ between any pixel (x, y) of the k-th bit-plane and each of its neighbours (along four main directions) is computed, and the distribution of these differences is calculated. This distribution is analysed in order to assess if it has been generated by a random or a textured intensity distribution (bit-plane). The bit-plane method has been applied to the CHIRS image in Fig.1, and its SNR has been computed.
The SNR spectrum of the same image has been also assessed applying the Scatter-plot approach (Aiazzi, 2002). This method computes a scatterplot of local estimates of mean-standard deviation

pairs computed by a moving window procedure. Evidently, the scatterplot is expected to contain a main cluster of point, elongated parallel to the local mean axis. The intercept to zero mean of this scatterplot main lobe is a fair estimate of the noise standard deviation, depurated from effects of image texture. In our procedure, this interpolation of the scatterplot main lobe is performed using the Hough transform representation of the scatterplot image. Supplementary information concerning this method can be found in barducci et al. (2005).
The SNR spectra as computed by the two considered algorithms are plotted in Fig.2.

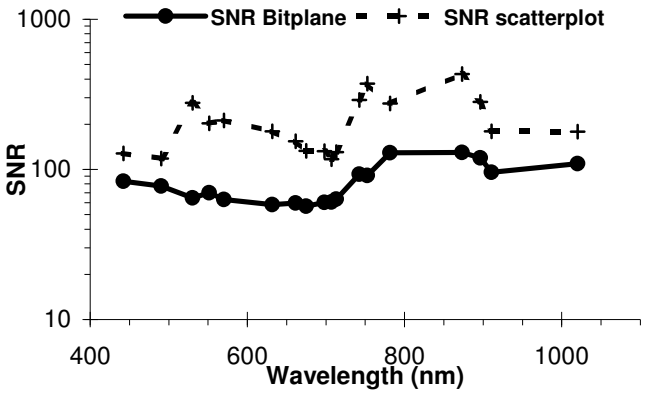

Fig. 2. SNR v.s. wavelengths obtained processing the CHRIS image of Fig.1 with bit-plane and scatterplot methods.

3. REFLECTANCE MAPS

3.1 Atmospheric effects correction

To retrieve spectral reflectance maps form remotely sensed images, a suitable model have to be implemented, taking into account the atmospheric effects. These include the absorptions and the scatterings by molecules and aerosols on the different components of the radiance reaching the sensor (Vermote, 1997) as depicted in Fig.3, where: 1. is the component not reflected by the ground and scattered both out and into the field of view of the sensor; 2.is the component not reflected by the ground and scattered only into the field of view of the sensor; 3. is the component reflected by the ground directly transmitted without scattering; 4. is the component reflected by the ground only scattered into the field of view of the sensor; 5. is the component reflected by the ground scattered both out and into the field of view of the sensor; 6. is the component reflected by the ground scattered only out the field of view of the sensor; 7.is the component due to the neighbour pixel contribute scattered into the field of view of the sensor; and 8. is the component due to the neighbour pixel contribute on the observed pixel brightness.

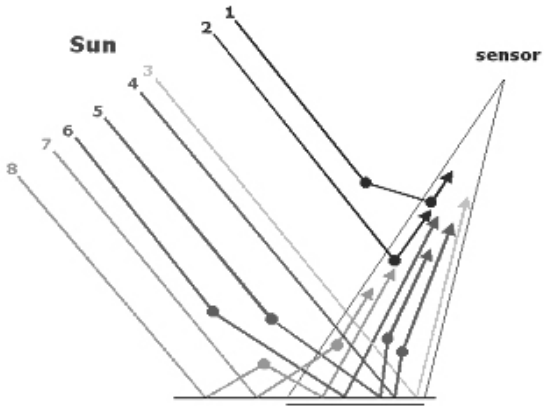

Fig. 3. Layout of the various components of the solar radiation propagating trough the atmosphere to ground and back to the sensor.

Supposing that light can be scattered only once and that the neighbourhood has spectral properties similar to the observed pixel, the Radiative Transfer Equation (RTE) may be solved using successive order method. Hence, an approximate solution is found and its expression differs from Eq.1 for an additional radiative contribution to the total irradiance impinging the surface. This general structure of the approximate solution is then utilised to find a solution to the RTE, which also includes multiple scattering, by comparing the surface reflectance simulated with MODTRAN with the expected one measured in laboratory. From this comparison three semi-empirical coefficients $A(z,\vartheta)$, α and $\beta(\vartheta)$ are found (Barducci, 2005) and the new solution obeys the following expression:

$$\rho(\lambda,\vartheta)=\frac{\pi\left[L_{1B}(\lambda,\vartheta)-L_{path}(\lambda,\vartheta)\right]}{E_{tot}(\lambda,\zeta)\left[T(\lambda,\vartheta)+\frac{A(z,\vartheta)}{2}\frac{1}{\lambda^{\alpha}}T^{\beta(\vartheta)}(\lambda,\vartheta)\right]}\frac{1}{\cos\vartheta} \tag{7}$$

The implicitly assumed approximation of an atmosphere with a plane-parallel geometry (see Eq.7) represents a standard method to solve complex mathematics without losing accuracy.

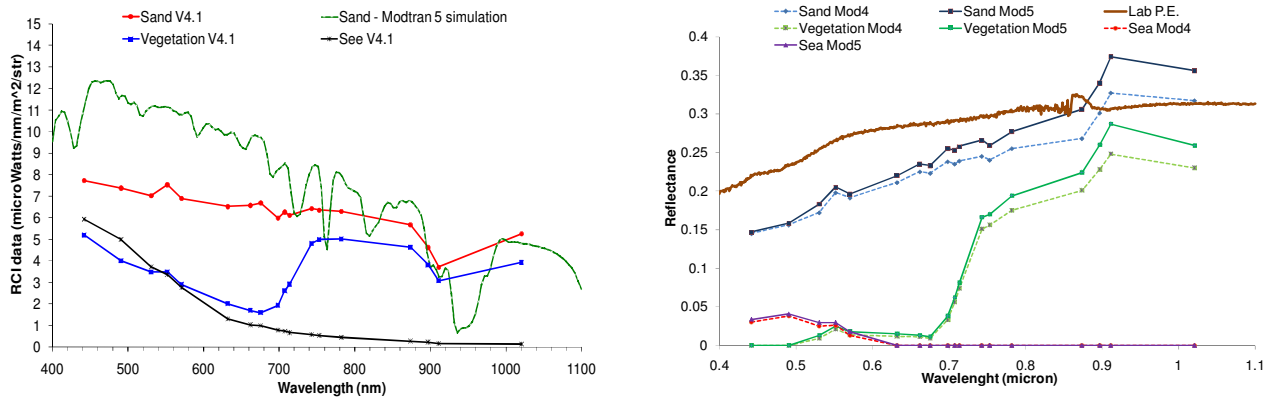

(a) *(b)*

Fig.4. September 18, 2003 acquisition over San Rossore at FZA=0: (a) RCI data release 4. Spectra are extracted from a sand pixel, a vegetation pixel (pine tree forest), and a sea pixel. Modtran 5 simulation is also reported for a sand pixel at nadir view.; (b) Reflectance spectra extracted from CHRIS image for the same sand pixel,a vegetation pixel (pine tree forest), and sea pixel using both MODTRAM 4.1 and MODTRAN 5 for atmospheric corrections..

Almost all atmospheric parameters included in Eq.7 were simulated by means of both Modtran 4 (Anderson, 1995) and Modtran 5 computer codes with exception of downwelling total spectral irradiance at ground that was in-field measured with a custom instrument described in a previous work (Barducci, 2004)

Single pixel Lambertian reflectance spectra assessed with this procedure from CHRIS data were compared with spectral measurements executed in laboratory over target samples taken from the corresponding point on the soil. We point out that due to the not negligible ground pitch of CHRIS pixels (roughly 18 m in our images) the related remotely sensed reflectance might be affected from sub-pixel spectral mixing phenomena.

In Fig.4a spectra for a sand pixel, a vegetation pixel (pine tree forest) and a sea pixel extracted from RCI release 4.1 image acquired on September 18, 2003 at FZA=0 are plotted. Modtran 5 simulation is also reported for a sand pixel at nadir view.. Reflectance spectra of the same reference pixels of Fig.4a are shown in Fig.4b using both Modtran 4 and Modtran 5 radiative trtansfer code for atmospheric corrections. Spectral reflectance of sand as measured in laboratory is also shown.

Figure 4b points out that reflectance spectra obtained using Modtran 5 are usually higher than the ones produced with Modtran 4. This is due to a better simulation of the aerosol contribution to the at sensor radiance.

3.1 Bi-directional Reflectance Distribution Function

If the assumption of a Lambertian surface doesn't hold true, we have to introduce the concept of BRDF, denoted symbolically as $\rho_{BRDF}(\lambda,\vartheta_0,\phi_0,\vartheta_r,\phi_r)$, which is defined as the ratio of the radiance $dL^{out}(\lambda,\vartheta_0,\phi_0,\vartheta_r,\phi_r;E_i)$ scattered into the direction (ϑ_r,ϕ_r) to the irradiance $dE_i(\lambda,\vartheta_0,\phi_0)$ impinging from the direction (ϑ_0,ϕ_0) within the element of solid angle $d\omega_0$ on a unitary surface area [11]:

$$\rho_{BRDF}(\lambda,\vartheta_0,\phi_0,\vartheta_r,\phi_r)=\frac{dL^{out}(\lambda,\vartheta_0,\phi_0,\vartheta_r,\phi_r;E_i)}{dE_i(\lambda,\vartheta_0,\phi_0)} \tag{8}$$

4. REMOTE SENSING CAMAPAIGNS: OUTCOMES FROM DATA PROCESSING

CHRIS long term series acquisitions allowed both multi-spectral and multi-temporal analysis continuously improving our understanding of different biogeochemical processes such as those involved in the change of vegetation status as observed in areas that are strongly affected by anthropogenic activities (Azzari, 1999). In particular CHRIS spatial and spectral resolution has allowed the estimation of narrow bands vegetation indexes like the Photo-chemical Reflectance Index (PRI).

In September 2004, preliminary estimates of canopy PRI and NDVI from CHRIS images were compared with leaf-level measurements from different plots corresponding to different vegetation types from among them some in wetlands.

LAI and hence NDVI is known to be correlated with fertility and light-use efficiency (Raddi, 2005), and this could explain the relationship with PRI. To this aim the following relationship are utilized:

$$PRI=\frac{(R_{531}-R_{570})}{(R_{531}+R_{570})} \qquad NDVI=\frac{(R_{782}-R_{675})}{(R_{782}+R_{675})}$$

where R is the surface reflectance at the given wavelength (in nm) indicated by the suffix.

The preliminary analysis of one CHRIS image, acquired on 8th September 2004 at 0° along track pointing angle, demonstrates the feasibility of PRI measurement from space. A good relationship was observed (Figure 5) between PRI measured at the leaf level as ground truth and PRI estimated from CHRIS imagery (R^2=0.45). The PRI_{ground} vs PRI_{CHRIS} is maintained also for the images at +36° and –36° along track pointing angles giving a R^2 of 0.69 and 0.41, respectively.

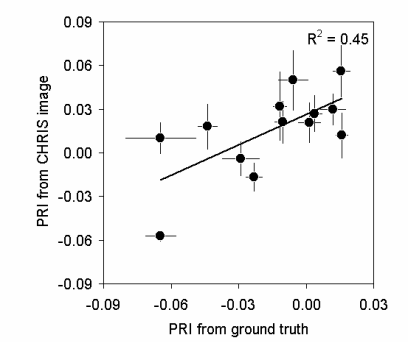

Fig. 5 Comparison of PRI measured in field the 8th September 2004 on 13 sampling areas and PRI retrieved from CHRIS image acquired the same day. Averages and standard deviations are reported for each area

Despite the noise of such a small signal, values are coherent across the image and differences among and within vegetation types are clearly visible, as displayed from a comparison of NDVI and PRI images in Figure 6 and 7, respectively.
In order to monitor seasonal changes in PRI and NDVI over the wet areas of Lame di Fuori Natural Reserve Area, CHRIS acquisitions on 27th March and 8th September 2004 are considered. The related results are displayed in Figure 6 and 7 for along track pointing angle of 0°, where changes in NDVI and PRI maps from early spring to late summer are reported. Seasonal changes in PRI and NDVI maps shown in figure 6 and 7 put in evidence the changes in land-use.

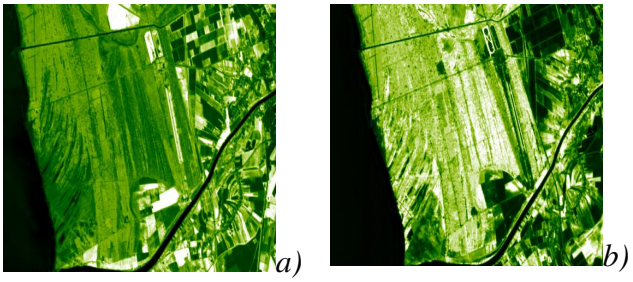

Fig.6 NDVI images computed from the CHRIS acquisition on March 27, 2004 at FZA=0° and MZA = 17° (a), and on September 8, 2004 at FZA=0° and MZA=11° (b). Bright pixels represent areas with high values of NDVI

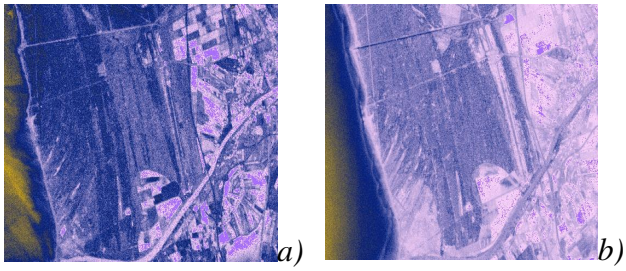

Fig.7 PRI images computed from the CHRIS acquisition on March 27, 2004 at FZA=0° and MZA=17° (a) and on September 8, 2004 at FZA=0° and MZA=11° (b). Dark pixel indicates areas with a low value of PRI.

Data collected during seven years allowed us to perform a multi-temporal analysis of the coastal area. In figure 8 an example of long term land change is reported. In Figure 8a an image of the coastal zone close Morto Nuovo channel mouth acquired on September 2003 is reported, while in figure 8b is reported an image of the same area acquired on September 2008. It is evident the coast erosion phenomena.

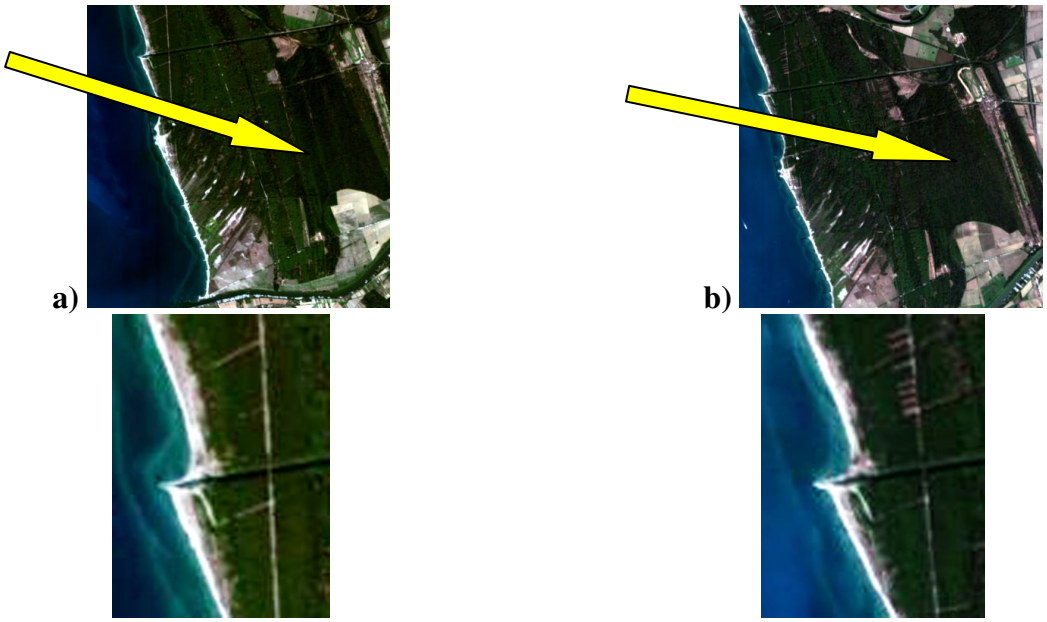

Fig. 8. Images of the coastal zone close Morto Nuovo channel mouth acquired on September 2003 (a) and on September 2008 (b)

5. CONCLUSIONS

The activities carried out along last years are revised and summarized. Firstly the data acquired by CHRIS over San Rossore (Italy) test site have been processed in order to suppress any disturbances, then the quality of these data have been assessed in term of SNR. The results of the atmospheric effects correction procedure as well as the retrieval and validation of some biogeochemical parameters are discussed.

In conclusion we can stress that CHRIS/PROBA is a very useful tool to allow the scientific users in quantitative remotely sensed measurements. At the same time the experience gained from this kind of instrumentation can help in the development of the new spaceborne imaging spectrometers.

6. REFERENCES

Aiazzi B., L. Alparone, A. Barducci, S. Baronti, I. Pippi, 2002."Estimating Noise and Information of Multispectral Imagery", *Optical Engineering*, Vol. 41, n. 3, pp. 656 – 668.

Anderson G.P., F.X. Kneizys, J.H. Chetwynd, J. Wang, M.L. Hoke, L.S. Rothman, L.M. Kimball, R.A. McClatchey, E.P. Shettle, S.A. Clough, W.O. Gallery, L.W. Abreu, J.E.A. Selby, 1995. "FASCODE / MODTRAN / LOWTRAN: Past / Present / Future", *18th Annual Review Conference on Atmospheric Transmission Models*, Hanscom AFB, MA, 6-8 June 1995.

Azzari M., Marcaccini P., Pizziolo G., 1999. A Geographical Information System in Tuscan Coastal Wetlands In *Actes du II Congres International sur la Science et la Technologie pour la Sauveguarde du Patrimoine Culturel dans les Pays du Bassin Méditerranéen* (Paris 5-9 juillet 1999), Paris, Elsevier, pp.1189-1192.

Barducci A., and I. Pippi, 2001. "Analysis and rejection of systematic disturbances in hyperspectral remotely sensed images of the Earth", *Applied Optics*, Vol. 40, pp. 1464 – 1477.

Barducci A. , F. Castagnoli, D. Guzzi, P. Marcoionni, I. Pippi, M. Poggesi, 2004. "Solar spectral irradiometer for validation of remotely sensed hyperspectral data", *Applied Optics*, 43, pp. 183 – 195.

Barducci A., D. Guzzi, P. Marcoionni, I. Pippi , 2005. "CHRIS Performance Evaluation: Signal-to-Noise Ratio. Instrument Efficiency, and Data Quality from Acquisitions over San Rossore (Italy)

Forestry Test Site". *3rd CHRIS / PROBA Workshop*, ESRIN, Frascati, 21-23 March 2005. Proceedings: ESA

Barducci A., D. Guzzi, P. Marcoionni, I. Pippi, 2005. "Atmospheric effects correction of Chris data acquired over san Rossore for their assimilation in biochemical models", *3rd CHRIS / PROBA Workshop*, ESRIN, Frascati, 21-23 March 2005. Proceedings: ESA

Cutter M. A. , L. S. Johns , D.R. Lobb , T.L. Williams , J.J. and Settle, 2003. "Flight Experience of the Compact High Resolution Imaging Spectrometer (CHRIS)", *Proceeding of SPIE Conference 5159 Imaging Spectrometry IX*, August 2003, San Diego, California, USA.

Raddi S., S. Cortes, I. Pippi, F. Magnani, 2005. "Estimation of vegetation photochemical processes: an application of the Photochemical Reflectance Index at the San Rossore test site", *3rd CHRIS / PROBA Workshop*, ESRIN, Frascati, 21-23 March 2005. Proceedings: ESA

Ramsey E., D. Chappell, S. Laine, G. Nelson, S. Sapkota, and T. Stoute ,1997. Identification of wetland zonation and inundation extent by using satellite remote sensing and ground-based measurements. In Proceedings of the *Fourth International Conference on Remote Sensing for Marine and Coastal Environments*, Vol. I, Orlando, Florida, 17-19 March 1997. Ann Arbor, Michigan. pp. 498-501.

Vermote E., N. El Saleous, C. Justice, Y. Kaufman, J. Privette, L. Remer, J. Roger, D. Tanré, 1997. "Atmospheric correction of visible to middle-infrared EOS-MODIS data over land surfaces: background, operational algorithm and validation", *Journal of Geophysical Research*, 102, pp. 17131 – 17142.